GdBCO bulk superconducting helical undulator for x-ray free-electron lasers

Marco Calvi [*], Sebastian Hellmann, Eduard Prat, Thomas Schmidt, and Kai Zhang [†]
Paul Scherrer Institute, Villigen PSI, Switzerland

Anthony R. Dennis and John H. Durrell
Department of Engineering, University of Cambridge, Trumpington Street, Cambridge, United Kingdom

Mark D. Ainslie
Department of Engineering, King's College London, Strand, London WC2R 2LS, United Kingdom

We report on the performance of a new type of helical undulator based on bulk single-grain $GdBa_2Cu_3O_{7-\delta}$ high-temperature superconductors. The 104-mm-long prototype with a period length of 16 mm and a magnetic aperture of 4 mm achieves an on-axis field above 2.5 T at a temperature of 10 K. This undulator technology has the potential to change the design parameters of future x-ray free-electron lasers, making them more compact and powerful.

X-ray free-electron lasers (FELs) are cutting-edge research tools employed in various scientific fields; such lasers allow the observation of matter on spatial and temporal scales of atomic processes. The FEL radiation is produced by a multi-GeV high-brightness electron beam traveling through a periodic array of magnets termed an undulator.

The central wavelength of the FEL radiation is defined by the resonance condition,

$$\lambda = \frac{\lambda_u}{2\gamma^2}\left(1 + \frac{K_x^2}{2} + \frac{K_y^2}{2}\right), \tag{1}$$

where λ_u is the period length of the undulator, γ is the Lorentz factor of the electron beam, and K_x and K_y are the undulator deflection parameters. Thus, K_x (K_y) is the maximum deviation angle on the yz plane (xz plane) when divided by the Lorentz factor, and it can be expressed as

$$K_x = \frac{e\lambda_u B_{x0}}{2\pi mc}, \tag{2}$$

where B_{x0} (B_{y0}) is the magnetic-field amplitude along the x axis (y axis), e and m are the charge and the mass of the electron, respectively, and c is the speed of light.

There are two primary types of undulators: planar, corresponding to linearly polarized light, and helical, providing circularly polarized radiation. Because it holds for both types,

*marco.calvi@psi.ch.
†Also at Zhangjiang Laboratory, Shanghai, 201210, China.

the definition of $K^2 = K_x^2 + K_y^2$ is used in this Letter. The magnetic field of a helical undulator has the following analytical expression [1]:

$$\begin{aligned} B_x(z) &= B_0 \sin(2\pi z/\lambda_u), \\ B_y(z) &= B_0 \cos(2\pi z/\lambda_u), \end{aligned} \tag{3}$$

where $B_0 = B_{x0} = B_{y0}$ and it is generally preferred since it induces a stronger FEL coupling between the electrons and photons, resulting in better FEL performance [2]. The FEL process saturates earlier and with higher powers with helical undulators. In other words, helical undulators correspond to more compact and high-power sources. For instance, experience at the soft x-ray beamline of Swiss FEL shows a 20 to 25% improvement in both saturation power and length when employing helical undulators. Compactness is an especially important feature for FELs since it allows reduction of the overall facility footprint and costs, thus, increasing the accessibility of this key technology to a larger scientific community.

There are currently five hard x-ray FEL facilities in operation worldwide: Linac Coherent Light Source [3], SPring-8 Angstrom Compact FEL [4], EuXFEL [5], Pohang Accelerator Laboratory [6], and SwissFEL [7]. The most compact and affordable facility is SwissFEL, producing hard x-ray radiation for 0.1 nm with the shortest undulator period (15 mm) and the lowest electron beam energy (6 GeV) [7]. All these x-ray FEL facilities use planar undulators. This is due to the lack of an established helical technology with the required magnetic properties. There is extensive worldwide research trying to make helical undulators suitable for hard x-ray FELs. For instance, efforts are ongoing to increase the strength of the APPLE undulators [8], moving the magnets into vacuum [9,10] and/or cooling them down to liquid-nitrogen temperature [11]. Furthermore, there is extensive research on superconducting helical undulators [12]. A notable example

is the work presented in Ref. [13] where a K of 1.22 was demonstrated for a period of 11.5 mm, but with a 1% peak to peak field variation that would require further optimization for its implementation in an x-ray FEL. Up to now, the only superconducting helical undulator in operation [14] is installed in the Advanced Photon Source (APS) at the Argonne National Laboratory (ANL). It features a K of 1.70 with a period length of 31.5 mm. According to Eq. (1), this device would require an electron-beam energy of about 10 GeV to lase at 0.1 nm at its maximum strength. For further information on superconducting undulators, we refer the reader to comprehensive state-of-the-art review in Ref. [15].

Here, we present the experimental results of a new type of helical undulator based on bulk single-grain $GdBa_2Cu_3O_{7-\delta}$ (GdBCO) high-temperature superconductors (HTS). We measured a record magnetic field above 2.5 T for a period of 16 mm, equivalent to a K value above 5. Such an undulator could produce hard x-ray FEL radiation with higher power and in a more compact beam line than presently employed planar configurations. For example, lasing at 0.1 nm becomes possible with electron-beam energies of 6 GeV as in the hard x-ray beam line of SwissFEL but with enhanced FEL performance. Our calculations, based on the Ming-Xie model [16] for SwissFEL parameters, show a power increase and an undulator length reduction of about 15 to 20% depending on the radiation wavelength.

We have previously [17] discussed the possibility that a helical superconducting undulator might be built implementing HTS bulks. Its design works on the principle of the superconducting staggered array undulator introduced by Kii and co-workers [18,19] where two rows of GdBCO bulks are magnetized by means of a solenoidal field. In this helical geometry, there are four rows of bulks: one pair generates the vertical magnetic-field component, whereas, the second pair generates the horizontal magnetic-field component. Thus, for simplicity's sake, it can be illustrated as the superposition of two classical staggered array undulators rotated 90° relative to the other. Following the research strategy proposed in Ref. [17], we first assembled a prototype of the hybrid staggered array where additional ferromagnetic shims were introduced both to increase the overall field and tune the local field strength. After reporting a record field of 2.1 T in this first planar undulator prototype [20], we assembled the same series of GdBCO bulks (from Nippon Steel Corporation) in a modified sample holder. Two half copper shells were precisely machined to hold the disks by means of two rows of screws one on each side, see Fig. 1(a). The helical magnetic configuration is obtained by stacking the disks one after the other (without space in between) where each of them is rotated around the beam axis 90° with respect to the previous one, see Fig. 1(b). This rotation must be always either clockwise or anticlockwise depending on the direction of circular photon polarization desired.

To precisely control the orientations of the bulk superconductor elements, four grooves lying on two perpendicular lines were machined along the length of the two half shells to match with the two tips of the disks corresponding to each of the four desired orientations. To minimize the geometrical errors, the GdBCO bulks were ground to a thickness of 4 ± 0.005 mm and precisely machined with electrical
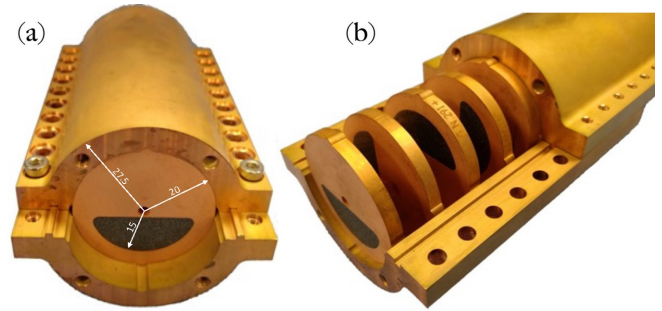

FIG. 1. The short helical undulator prototype used for the measurements presented herein. On the left, (a) the closed structure where the Cu-GdBCO disks are bolted between two copper shells. The four grooves (up/down-left/right) used for the precise alignment of the disks are clearly distinguishable. On the right, (b) the details of the orientation of the disks are shown for clarification with an additional spacing in between them. In the actual testing configuration, the disks are in close contact. Dimension units are in millimeters.

discharge machining wire erosion to obtain the final half moon shape with an accuracy better than 5 μm. This precision is also required to systematically achieve the prestress induced by the copper sleeves mandatory to reduce the tensile stress generated by the large currents, see details in Ref. [20], and to maximize the cooling by conduction. To summarize, this prototype consists of 26 Cu-GdBCO bulk disks, corresponding to 6.5 periods each of 16-mm length, which generates an antisymmetric magnetic-field profile. ANSYS simulations [21] were performed following the critical state model [22], which confirmed the expected shape of the field profile and predicted amplitude larger than 2.5 T.

The measurement campaign was performed at the University of Cambridge in the Royce Institute 12-T vertical superconducting solenoid using the same equipment as described in Ref. [20]: a heater in a closed loop with a thermometer to control the temperature of the prototype, cooled in a stream of cold-helium gas, and a set of five Hall sensors driven by an external linear stage to scan the three components of the magnetic-field profile along the undulator axis. The prototype was field cooled at 10 T down to 10 K. The external magnetic field was reduced with a constant rate of 1 T/h down to zero and the on-axis magnetic-field profiles were tentatively measured every tesla to monitor the evolution of the undulator field. The recorded undulator magnetic-field profiles are presented in Fig. 2 where the two components of the field B_x and B_y are presented for different magnetization levels. They are phase shifted by 90° and antisymmetric as expected from the simulation results. Because the profiles deviate from a perfect periodic signal, B_{x0} and B_{y0} are defined as the average amplitude of the, respectively, ten central peaks and σ_B as their standard deviation to account for the field errors.

Figure 3 shows a summary of the magnetic measurement results. The field strength increases linearly with the solenoidal field up to 5 T when the slope decreases until a clear sign of saturation starts above 8 T. The maximum measured B_0 is 2.57 T, corresponding to a K of 5.43. Nevertheless, full saturation is not reached, even at the end of the charging process, giving room for slightly higher fields
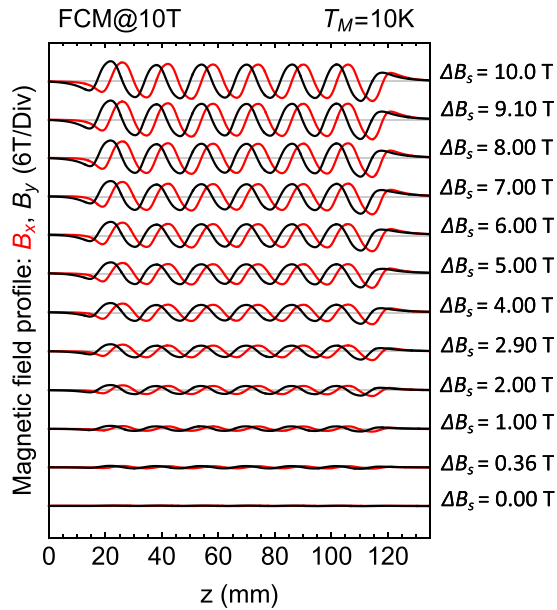
FIG. 2. The measured magnetic-field profiles of the two transversal components of the undulator field B_x and B_y as a function of the variation of the external solenoidal field $10\,\text{T} - \Delta B_s$ and at the magnetization temperature $T_M = 10\,\text{K}$.

FIG. 3. Summary of the magnetic measurement results on the helical undulator. On the left axis, the magnetic-field amplitude of the undulator (B_0) as a function of the variation of the external solenoidal field; on the right axis, the field errors evaluated as the standard deviation of the field amplitude of the central ten peaks.

in future experiments. A 2.3% peak-to-peak variation is very satisfactory and comparable to more standard permanent magnet undulators. As for these latter undulators, a procedure for further improving the phase error and the straightness of the electron trajectory is required.

In conclusion, we have presented a record magnetic field for a helical undulator of 2.57 T for a period length of 16 mm and a magnetic aperture of 4-mm diameter. This helical undulator outperforms any previous device presented in the literature up to now. By scaling our results to shorter periods, it is expected to obtain a K above 1 even for an 8-mm period length, which would allow lasing at 0.1 nm with only 4.0 GeV energies and with the advantage of the helical configuration. Our results represent a fundamental step change in undulator technology with tremendous consequences for x-ray FEL designs, making these facilities significantly more compact, affordable, and efficient than today.
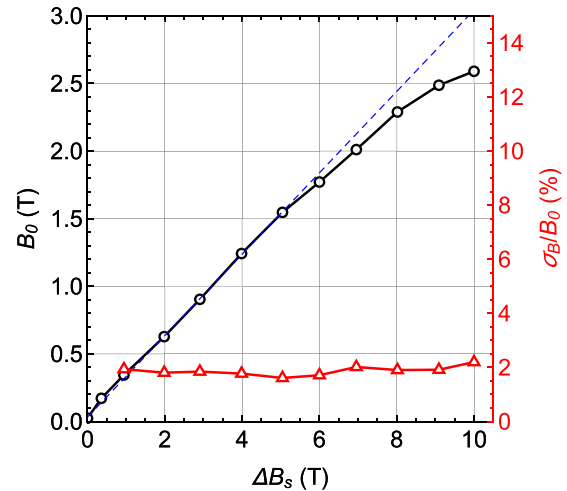
This first experimental proof of principle was carried out reusing the components arranged for the prototype of an undulator designed for the I-TOMCAT beam line [23], a new source for microscopy tomography planned in the upgrade of the Swiss Light Source (SLS2.0, [24]). As resource permits, an optimized design will be calculated and new components manufactured. This will allow shorter periods down to 8 mm and the use of ferromagnetic shims to fine-tune the local field amplitude. These improvements, together with sorting algorithms [25], will reduce further the level of the phase error but the quality required for the state-of-the-art FELs has to be demonstrated ($< 10°$).

[1] P. Schmüser, M. Dohlus, J. Rossbach, and C. Behrens, One-Dimensional Theory of the High-Gain FEL, in *Free-Electron Lasers in the Ultraviolet and X-Ray Regime*, Springer Tracts in Modern Physics, Vol. 258 (Springer International Publishing, Cham, 2014), pp. 39–61.

[2] C. Pellegrini, A. Marinelli, and S. Reiche, The physics of x-ray free-electron lasers, Rev. Mod. Phys. **88**, 015006 (2016).

[3] P. Emma *et al.*, First lasing and operation of an ångstrom-wavelength free-electron laser, Nat. Photonics **4**, 641 (2010).

[4] T. Ishikawa *et al.*, A compact x-ray free-electron laser emitting in the sub-ångström region, Nat. Photonics **6**, 540 (2012).

[5] W. Decking *et al.*, A MHz-repetition-rate hard X-ray free-electron laser driven by a superconducting linear accelerator, Nat. Photonics **14**, 391 (2020).

[6] H.-S. Kang *et al.*, Hard x-ray free-electron laser with femtosecond-scale timing jitter, Nat. Photonics **11**, 708 (2017).

[7] E. Prat *et al.*, A compact and cost-effective hard x-ray free-electron laser driven by a high-brightness and low-energy electron beam, Nat. Photonics **14**, 748 (2020).

[8] M. Calvi, C. Camenzuli, E. Prat, and T. Schmidt, Transverse gradient in Apple-type undulators, J. Synchrotron Radiat. **24**, 600 (2017).

[9] J. Bahrdt and S. Grimmer, In-vacuum APPLE II undulator with force compensation, in *13th International Conference on Synchrotron Radiation Instrumentation (SRI2018)*, AIP Conf. Proc. No. 2054 030031 (AIP, Melville, NY, 2019).

[10] J. Bahrdt, J. Bakos, S. Gaebel, S. Gottschlich, S. Grimmer, C. Kuhn, S. Knaack, F. Laube, A. Meseck, C. Rethfeldt, E. Rial, A. Rogosch-Opolka, M. Scheer, and P. Volz, The status of the in-vacuum APPLE II undulator IVUE32 at HZB / BESSY II, in *Proc. 13th International Particle Accelerator Conference (IPAC2022)* (JACoW Publishing, Geneva, Switzerland, 2022), pp. 2716–2718.

[11] E. C. M. Rial, J. Bahrdt, S. Grimmer, A. Meseck, and M. Scheer, Development of a cryogenic APPLE CPMUE15 at BESSY II, J. Phys.: Conf. Ser. **2380**, 012018 (2022).

[12] L. R. Elias and J. M. Madey, Superconducting helically wound magnet for the free-electron laser, Rev. Sci. Instrum. **50**, 1335 (1979).

[13] D. J. Scott, J. A. Clarke, D. E. Baynham, V. Bayliss, T. Bradshaw, G. Burton, A. Brummitt, S. Carr, A. Lintern, J. Rochford, O. Taylor, and Y. Ivanyushenkov, Demonstration of a High-Field Short-Period Superconducting Helical Undulator Suitable for Future TeV-Scale Linear Collider Positron Sources, Phys. Rev. Lett. **107**, 174803 (2011).

[14] M. Kasa, M. Borland, L. Emery, J. Fuerst, K. C. Harkay, Q. Hasse, Y. Ivanyushenkov, W. Jansma, I. Kesgin, V. Sajaev, Y. Shiroyanagi, Y. P. Sun, and E. Gluskin, Development and operating experience of a 1.2-m long helical superconducting undulator at the Argonne Advanced Proton Source, Phys. Rev. Accel. Beams **23**, 050701 (2020).

[15] K. Zhang and M. Calvi, Review and prospects of world-wide superconducting undulator development for synchrotrons and FELs, Supercond. Sci. Technol. **35**, 093001 (2022).

[16] M. Xie, Design optimization for an x-ray free electron laser driven by SLAC linac, in *Proceedings of the 1995 Particle Accelerator Conference, Dallas, Texas, USA, 1995* (IEEE, Piscataway, NJ, 1996), p. 183.

[17] M. Calvi, M. D. Ainslie, A. Dennis, J. H. Durrell, S. Hellmann, C. Kittel, D. A. Moseley, T. Schmidt, Y. Shi, and K. Zhang, A GdBCO bulk staggered array undulator, Supercond. Sci. Technol. **33**, 014004 (2019).

[18] T. Kii, H. Zen, N. Okawachi, M. Nakano, K. Masuda, H. Ohgaki, K. Yoshikawa, and T. Yamazaki, Design study on high-Tc superconducting micro-undulator, in *Proceedings of FEL 2006, BESSY, Berlin, Germany* (FEL, Berlin, 2006).

[19] R. Kinjo, M. Shibata, T. Kii, H. Zen, K. Masuda, K. Nagasaki, and H. Ohgaki, Demonstration of a high-field short-period undulator using bulk high-temperature superconductor, Appl. Phys. Express **6**, 042701 (2013).

[20] K. Zhang, A. Pirotta, X. Liang, S. Hellmann, M. Bartkowiak, T. Schmidt, A. R. Dennis, M. D. Ainslie, J. H. Durrell, and M. Calvi, Record field in a 10 mm-period bulk high-temperature superconducting undulator, Supercond. Sci. Technol. **36** 05LT01 (2023).

[21] K. Zhang, M. Ainslie, M. Calvi, S. Hellmann, R. Kinjo, and T. Schmidt, Fast and efficient critical state modelling of field-cooled bulk high-temperature superconductors using a backward computation method, Supercond. Sci. Technol. **33**, 114007 (2020).

[22] C. P. Bean, Magnetization of Hard Superconductors, Phys. Rev. Lett. **8**, 250 (1962).

[23] SLS 2.0 Beamline Conceptual Design Report, PSI-Bericht 21-01, 378 (2021).

[24] A. Streun, T. Garvey, L. Rivkin, V. Schlott, T. Schmidt, P. Willmott, and A. Wrulich, SLS-2 – the upgrade of the Swiss Light Source, J. Synchrotron Radiat. **25**, 631 (2018).

[25] R. Kinjo, M. Calvi, K. Zhang, S. Hellmann, X. Liang, T. Schmidt, M. D. Ainslie, A. R. Dennis, and J. H. Durrell, Inverse analysis of critical current density in a bulk high-temperature superconducting undulator, Phys. Rev. Accel. Beams **25**, 043502 (2022).